4.1 The structure and evolution of vortex lines in supercell thunderstorms

PAUL MARKOWSKI*AND YVETTE RICHARDSON

Department of Meteorology, Pennsylvania State University, University Park, PA

1. Introduction

Vortex lines have been analyzed relatively infrequently within the severe storms community, and when they have been shown, often they only are presented schematically within conceptual models (e.g., to illustrate the vorticity tilting process responsible for midlevel mesocyclogenesis). We recently have been looking at vortex lines in observed and simulated supercell thunderstorms. Is there anything that can be gleaned about the processes associated with the amplification of low-level rotation from examining vortex lines?

In our oral presentation, we focus on the vortex line "arches" that emanate from the low-level mesocyclones of supercells (both tornadic and nontornadic). The oral presentation summarizes the idealized simulation and observational findings presented in recent articles by Straka et al. (2007) and Markowski et al. (2008). Also discussed in the oral presentation is the kinematic and probable dynamic similarity of the vortex line arches observed in supercells to those observed in larger-scale convective systems in conjunction with line-end vortices. Moreover, we present some speculations about why tornadogenesis is favored in supercell environments that have high relative humidity in the boundary layer and strong low-level shear.

Given the time constraints, our oral presentation does include a discussion of the evolution of vortex lines that precedes the development of vortex line arches. The discussion is presented below instead.

2. Evolution of vortex lines in a supercell thunderstorm

A numerical model is used to investigate the evolution of vortex lines from shortly after initiation, when a deep, buoyant updraft is present but before outflow is observed at low levels, through the time at which strong rotation and substantial horizontal buoyancy gradients are found near the surface. (Rainfall and low-level outflow is extensive by the time mobile radars typically would commit to or arrive at a storm; thus, observations of vortex lines early in a storm generally are unavailable.) The Bryan cloud model is used (Bryan and Fritsch 2002) to produce a cyclonically rotating, rightward-propagating supercell. The model is initialized with the Weisman and Klemp (1982) thermodynamic profile and the Rotunno and Klemp (1982) clockwise-turning hodograph. The horizontal and vertical grid spacing are 500 m and 250 m, respectively. The NASA-Goddard version of the Lin et al. (1983) microphysics parameterization is used. There are no surface fluxes or radiative transfer processes.

Vortex lines are drawn through and in close proximity to the maximum vertical vorticity at 0.5 km, 2.5 km, and 5.0 km in Figs. 1–4. One of the primary limitations of vortex lines is that they do not behave as material lines in regions of baroclinic vorticity generation. Baroclinic vorticity generation is significant in many parts of the storm, e.g., within the outflow and within the updraft itself (there would not be a buoyant updraft in the first place without horizontal density gradients). Although it is not possible to track specific vortex lines in time—it is not possible to know whether a vortex line observed at one time is the same one observed a little earlier or later—vortex line analyses still can be enlightening in that they can suggest plausible methods of vorticity generation and reorientation (e.g., observations of vortex rings might lead one to surmise that a local buoyancy extremum is present and responsible for the generation of the rings).

At $t = 20$ min, all of the vortex lines passing through the vertical vorticity maxima at 0.5 km, 2.5 km, and 5.0 km originate in the ambient environment (Fig. 1). No outflow is present at the surface at this early time, although a deep, intense updraft extends from the lifting condensation level to the upper troposphere. Some of the vortex lines coil around the buoyant midlevel updraft as a result of baroclinic vorticity generation on the flanks of the updraft.

Outflow is observed at the surface by $t = 40$ min, at which time all of the vortex lines that contribute to the vertical vorticity maximum at 0.5 km can be traced into the cold pool (Fig. 2). The orientation of the low-level vortex lines is parallel to the buoyancy isopleths within the outflow, suggesting that the vortex lines passing through and near to the vertical vorticity maximum at 0.5 km have been strongly influenced by baroclinic vorticity generation. A few of these vortex lines exit the cold pool and enter the environment east of the storm (i.e., environmental vortex lines are deflected to the left by westward baroclinic vorticity generation along the forward flank of the storm). At this time there is a clear difference between the vortex lines that pass through and near the midlevel (2.5 and 5.0 km) vertical vorticity maxima and the low-level (0.5 km) vertical vorticity maximum. Unlike the vortex lines that pass through and near the low-level vorticity maximum, the vortex lines that pass through the midlevel vertical vorticity maxima can be traced back into the environment (Fig. 2).

By $t = 80$ min, a mature supercell is established, with significant rotation extending all the way to the lowest grid level (125 m). (Obviously downdrafts have played a critical role in enabling the storm to achieve this state.) Vortex lines passing through the vertical vorticity maxima at 2.5 and 5.0 km

**Corresponding author address*: Dr. Paul Markowski, Department of Meteorology, Pennsylvania State University, 503 Walker Building, University Park, PA 16802; *e-mail*: pmarkowski@psu.edu.

come from the environment *and* from near the ground within the outflow (where baroclinic generation is important) (Fig. 3). Thus, the "midlevel" and "low-level" mesocyclone distinctions, which traditionally have been based on whether environmental vorticity or internally generated baroclinic vorticity is tilted, are problematic (moreover, the adjective "low-level" and the point at which vertical vorticity is large enough to identify a circulation as a "mesocyclone" are subjective anyway).

Many of the vortex lines that pass through the vertical vorticity maximum at 0.5 km at $t = 80$ min form arches (Fig. 4). Vortex lines arches also are found in supercells for which dual-Doppler observations exist. As indicated above, the oral presentation focuses on what vortex lines arches might tell us about the process associated with the development of rotation near the ground in supercells.

3. Summary

We break the lifecycle of a supercell into three stages in terms of the vortex line configurations. In the first stage (in roughly the first 30 min following initiation), a nascent supercell without low-level outflow tilts environmental vortex lines to generate vertical vorticity. Vertical vorticity generation from tilting is positive everywhere above the ground. Tilting vanishes at the ground and is a maximum at the level where the product of the environmental wind shear and horizontal updraft gradient is largest. Significant vertical vorticity (i.e., $\sim 10^{-2}$ s^{-2}) generally is confined to midlevels, although in a case of very large vertical shear and CAPE, tilting by an updraft alone can yield significant vertical vorticity even as low as 0.5–1.0 km. In the second stage (roughly 30–60 min after initiation), low-level outflow and baroclinic generation/modification of low-level vortex lines is present and significant vertical vorticity exists from the surface to the upper reaches of the storm. The vortex lines that pass through the midlevel vertical vorticity maxima originate in the environment as they did in the first stage, but the vortex lines the pass through the low-level vertical vorticity maximum originate or have been strongly modified by the cold pool. By the third stage (roughly 60 min after initiation and beyond), the low-level vortex lines are "drawn" farther upward, forming prominent arches. Some of the vortex lines that pass through the low-level vertical vorticity maximum extend all the way to the storm summit, passing through the midlevel vertical vorticity maxima along the way. Thus, the vortex lines that pass through the midlevel vertical vorticity maxima in this stage originate in both the environment and the cold pool. In other words, the midlevel mesocyclone of a mature supercell has vorticity contributions from the tilting of environmental horizontal vorticity as well as from the upward advection of vertical vorticity from near the ground, which ultimately has its roots within the cold pool via baroclinic vorticity generation.

Acknowledgments. We are grateful for the discussions with our collaborators Drs. Bob Davies-Jones, David Dowell, Erik Rasmussen, Jerry Straka, Jeff Trapp, and Josh Wurman. Support from NSF grants ATM-0338661, ATM-0437512, ATM-0644533, and ATM-0801035 also is acknowledged.

REFERENCES

Bryan G. H., and J. M. Fritsch, 2002: A benchmark simulation for moist nonhydrostatic numerical models. *Mon. Wea. Rev.*, **130**, 2917–2928.

Lin, Y.-L., R. D. Farley, and H.D. Orville, 1983: Bulk parameterization of the snow field in a cloud model. *J. Appl. Meteor.*, **22**, 1065–1092.

Markowski, P. M., J. M. Straka, E. N. Rasmussen, R. P. Davies-Jones, Y. Richardson, and J. Trapp, 2008: Vortex lines within low-level mesocyclones obtained from pseudo-dual-Doppler radar observations. *Monthly Weather Review*, **136**, 3513–3535.

Rotunno, R., and J. B. Klemp, 1982: The influence of the shear-induced pressure gradient on thunderstorm motion. *Mon. Wea. Rev.*, **110**, 136-151.

Straka, J. M., E. N. Rasmussen, R. P. Davies-Jones, and P. M. Markowski, 2007: An observational and idealized numerical examination of low-level counter-rotating vortices toward the rear flank of supercells. *Electronic Journal of Severe Storms Meteorology*, **2(8)**, 1–22.

Weisman, M. L., and J. B. Klemp, 1982: The dependence of numerically simulated convective storms on vertical wind shear and buoyancy. *Mon. Wea. Rev.*, **110**, 504–520.

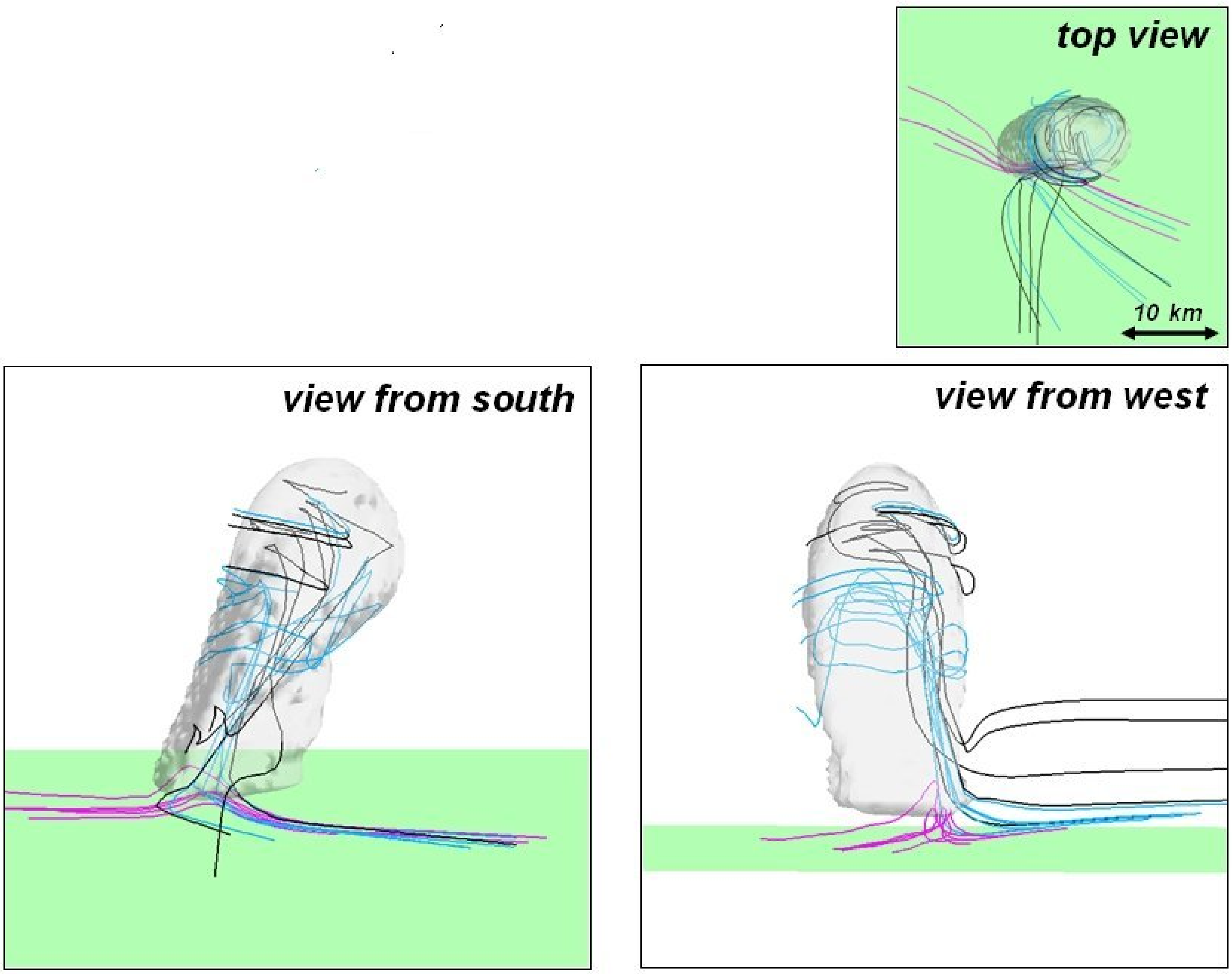

FIG. 1. Vortex lines draw through and in close proximity to the maximum vertical vorticity at 0.5 km (magenta), 2.5 km (blue), and 5.0 km (black) at $t = 20$ min. The translucent isosurface is the cloud.

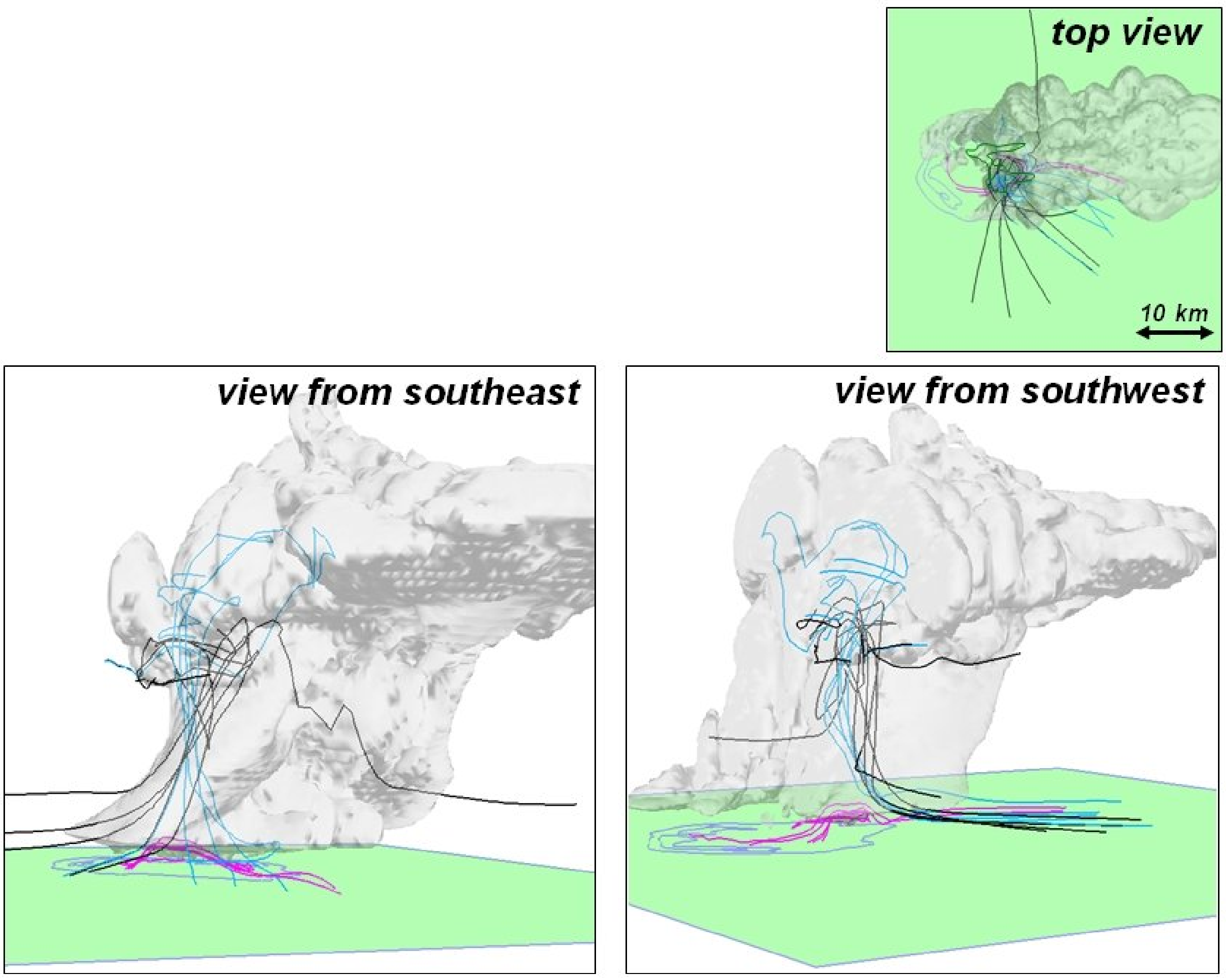

FIG. 2. As in Fig. 1, but for $t = 40$ min. The gust front (the $\theta' = -1$ K contour; dark blue) and rainwater ($q_r = 0.001$ g kg^{-1}; dark green) field also are shown in the top view.

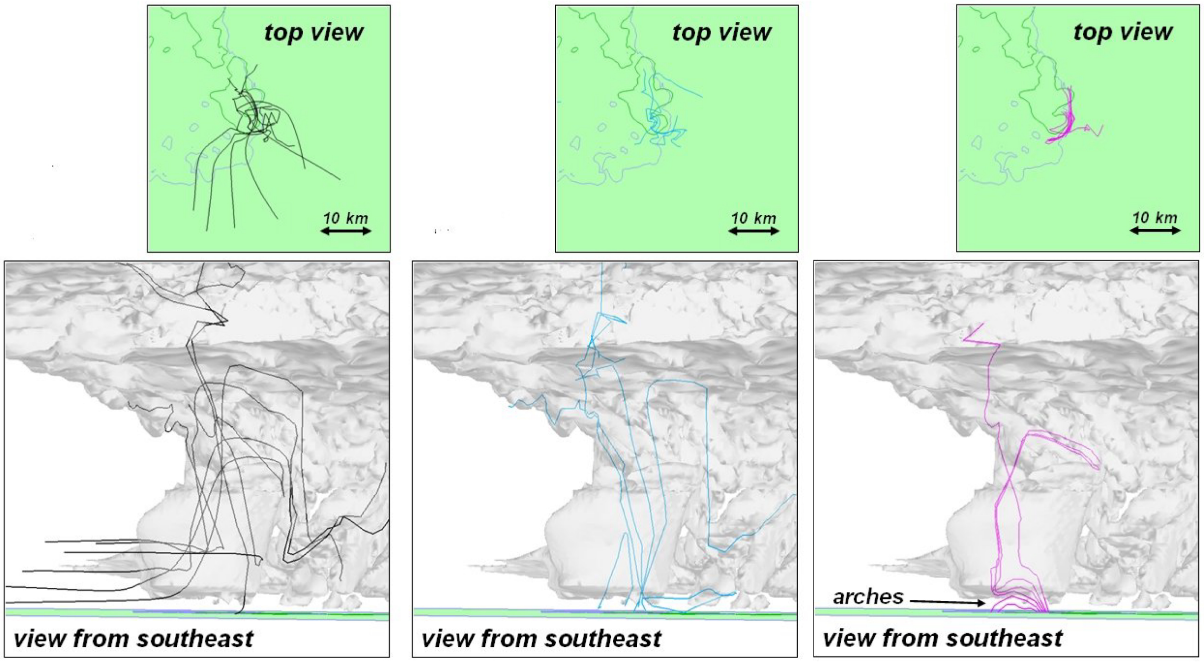

FIG. 3. As in Figs. 1 and 2, but for $t = 80$ min. The vortex lines passing through and near to the vorticity maxima at 0.5, 2.5, and 5.0 km are shown in separate panels in order to make the figure more readable. The gust front (the $\theta' = -1$ K contour; dark blue) and rainwater ($q_r = 0.001$ g kg^{-1}; dark green) field also are shown in the top views.

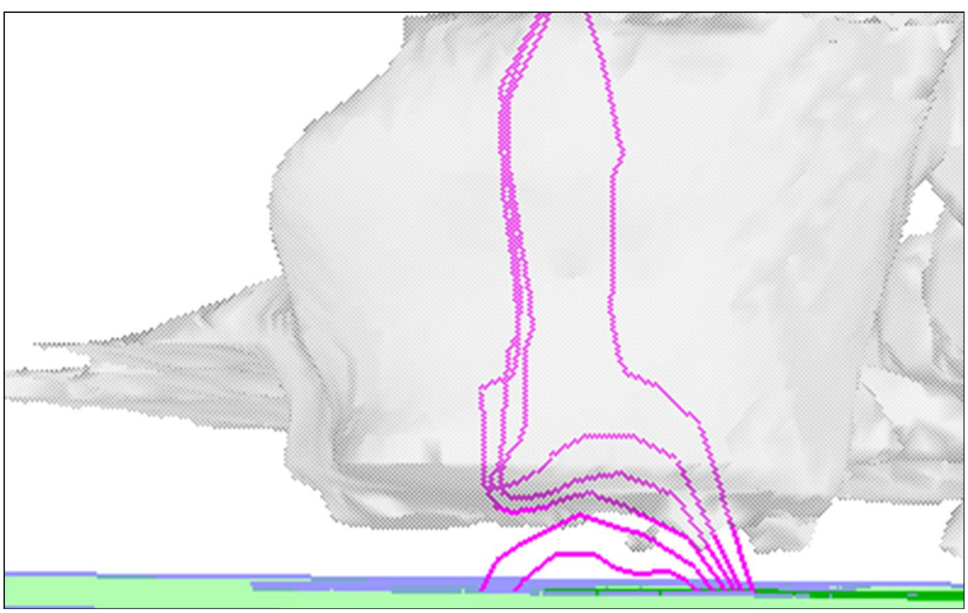

FIG. 4. Zoomed in view of the vortex lines passing through and near to the vertical vorticity maximum at 0.5 km at $t = 80$ min. The view is from the same vantage point as Fig. 3.